Supplementary Information (SI) for ChemComm.

Supplementary Information

Spatial Confinement Boosts C–C Coupling in Brushed Cu/Ag@CuO NWs for CO_2 Electroreduction into C_2H_4

Chengbin Zhang[†], Wenya Fan[†], Peipei Li[†], Changjing Wang, Mengqian Li, Zequn Han, Qingxia Chen[*], and Xingchen Jiao[*]

Key Laboratory of Synthetic and Biological Colloids, Ministry of Education, School of Chemical and Material Engineering, Jiangnan University, Wuxi 214122, China.

[†]These authors contributed equally to this work.

Email: qxchen@jiangnan.edu.cn; xcjiao@jiangnan.edu.cn

EXPERIMENTAL SECTION

Synthesis of Cu NWs. The synthesis of Cu NWs was carried out according to the previous report[1] with some modifications. Briefly, 0.855 g of $CuCl_2 \cdot 2H_2O$, 0.99 g of glucose, and 5.4 g of HDA were completely dissolved in 400 mL of ultra-purified H_2O. This resulting homogeneous solution was then transferred into a 500 mL blue bottle, which was subsequently placed in an oil bath preheated to 50°C with magnetic stirring for 8 h. Following this, the temperature was raised to 70°C and maintained for 24 h. Subsequently, the solution was further heated to 100°C and kept for another 24 h. After the heating process, the bule bottle was take out. For the purification process, 20 mL of the above solution was centrifuged at 10000 rpm for 10 min, and the sediment at the bottom was evenly redispersed in 20 mL of H_2O. This homogeneous solution was then mixed with 20 mL of $CHCl_3$, shaken well, and left to stand for 30 min. After allowing the mixture to settle, the lower suspension was collected and centrifuged at 8000 rpm for 3 min. The precipitate obtained from centrifugation was washed three times with 20 mL of ethanol. Finally, the precipitate was evenly dispersed in an ethanol solution and stored in a refrigerator.

Synthesis of Cu/Ag@CuO NWs-D and Cu/Ag@CuO NWs-S. A concentrated $NH_3 \cdot H_2O$ solution was diluted with H_2O at a ratio of 5:1 and then added dropwise to a moderately concentrated $AgNO_3$ solution. The addition was continued until the initial precipitate formed in the $AgNO_3$ solution completely dissolved, preparing a solution of $[Ag(NH_3)_2]OH$. The previously synthesized Cu NWs were redispersed in ethanol. To this Cu NWs solution, drops of the prepared $[Ag(NH_3)_2]OH$ solution were added while maintaining a concentration of 1.0 mM. The mixture was stirred using a magnetic stirrer at room temperature for 30 min. After the reaction, the resulting precipitate was washed three times using ethanol and H_2O alternately, and then dried in a freeze dryer for 24 h. This procedure yielded Cu/Ag@CuO NWs-D. To produce Cu/Ag@CuO NWs-S, the duration of magnetic stirring was shortened.

Electrochemical Measurements. The electrochemical measurements of CO_2RR were carried out in a flow cell system (CX-Flow Cell, 10X10 mm) on a VSP-300 Potentiostat workstation (CHI760E C23460d) with a current amplifier (CHI680D C23643). Ag/AgCl electrode (saturated in 3.0 M KCl) and Ni mesh were employed as the reference and anode electrode, respectively. Catalyst-deposited gas diffusion electrode (GDEs, YLS-30T) was used as the cathode electrode. The cation exchange membrane (Fumasep FAA-3-50) was selected to separate the cathode and anode chambers. The peristaltic pump (BT100-2J, Longer Pump) was applied to circulate the catholytes (25 mL, 1.0 M KOH) and anolytes (25 mL, 1.0 M KOH) with the flow rate of electrolytes kept at 20 mL min^{-1}. Gaseous CO_2 (99.999%, purchased from Wuxi XinXiYi Technology Co., Ltd.) was passed through the cathode chamber with a flow rate of 30 sccm monitored by a gas mass flow controller (C100L, Sierra) during the whole CO_2RR measurements. The electrochemical impedance spectroscopy (EIS) was recorded on CHI760E electrochemical workstation utilizing a three-electrode configuration in CO_2-saturated alkaline solution with a VoltaLab potentiostat (PGZ-301).

Evaluation of CEE. The cathodic energy efficiency (CEE) is the percentage of chemical energy contained in the reduction product to the total input electrical energy, which is calculated as follows[2].

$$CEE = \frac{E_{OER}^{0} - E_{C2H4}^{0}}{E_{OER}^{0} - E_{applied}^{0}} \times FE_{C2H4} \times 100\%$$

Where CEE is the cathodic energy efficiency, E_{OER}^{0} is the standard electrode potential for anodic oxygen evolution reaction (1.23 V), and E_{C2H4}^{0} is the standard electrode potential for the reduction reaction of the cathode target product C_2H_4 (0.08 V). $E_{applied}^{0}$ is the applied potential and FE_{C2H4} is the Faraday efficiency of C_2H_4.

Table S1 lists the number of electrons transferred and the standard reduction potentials for each product in CO_2RR.

Characterizations. TEM images were performed with a HT7800 TEM with an acceleration voltage of 200 kV. HRTEM images and the corresponding EDS data were collected on a Talos F200X G2 TEM/STEM with a spherical aberration corrector. XRD patterns were obtained from a Philips X'Pert Pro Super diffractometer with Cu Kα radiation (λ = 1.54178 Å). Inductively coupled plasma spectrometry (ICP) with an Optima 7300 DV (ThermoScientific PlasmaQuad 3) was used to determine the elemental analysis of Cu and Ag in the catalysts. XPS spectra were acquired on an ESCALAB MKII system with Al Kα (hv = 1486.6 eV) as the excitation source. The binding energies obtained in the XPS spectral analysis were corrected for specimen charging by referencing C 1s to 284.8 eV. In situ FTIR spectra were obtained by using a Thermo Scientific Nicolet iS50. Liquid-phase products were determined and quantified by the nuclear magnetic resonance (Bruker, AVANCE III HD 400 MHz). The gas-phase products were analyzed with the gas chromatography (GC, Agilent 8860). Flow cell was commercially available from CX (CX-Flow Cell, 10×10 mm).

COMSOL Multiphysics Simulations. The finite element method (FEM) simulations were conducted through COMSOL Multiphysics v 6.2. The 2D axisymmetric component was constructed for simulation, and the geometric parameters of the model are shown in New Figure S*. The Electric Currents (e_c) and Transport of Diluted Species (t_{ds}) physics modules in COMSOL Multiphysics were used to couple the mass transfer of CO_2 with the electrode surface reaction to simulate and calculate the model CO_2 concentration distribution in electrolytes. The infinite element domain in the model was set to mapped meshing, and other meshes were set to free trihedral meshing. The relative tolerance in the steady-state solver was set to 0.01.

The concentration distribution of CO_2 presents a dynamic equilibrium. Following the mass transfer equation and Nernst equation:

$$\nabla \cdot J_j + \mu \cdot \nabla c_j = R_j$$

$$J_j = -D_j \nabla c_j - z_j u_{m,j} F c_j \nabla V$$

Where J_j is the total flux of the substance, R_j is the reactive source of the electrolyte solution, D_j is the diffusion coefficient (D_{CO2} is set to 1.6×10^{-9} m^2 s^{-1}), c_j is the concentration of ions, z_j is the number of charges, $u_{m,j}$ is the migration rate, F is the faradaic constant, and V is the potential of the electrode in the electrolyte.

Supplementary Figures

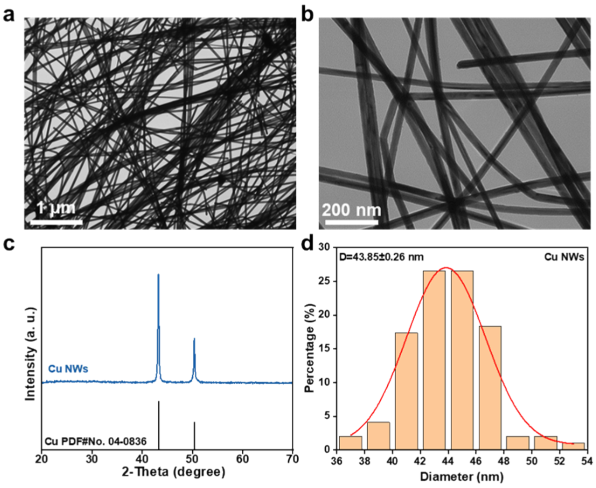

Figure S1. Morphological and structural characterizations of Cu NWs. (a-b) TEM images. (c) XRD pattern. (d) Histogram of the diameter.

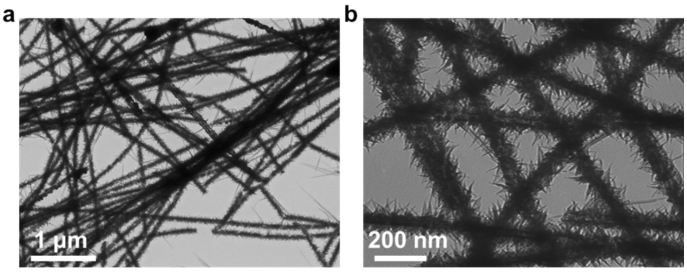

Figure S2. TEM images of Cu/Ag@CuO NWs-D with different magnifications.

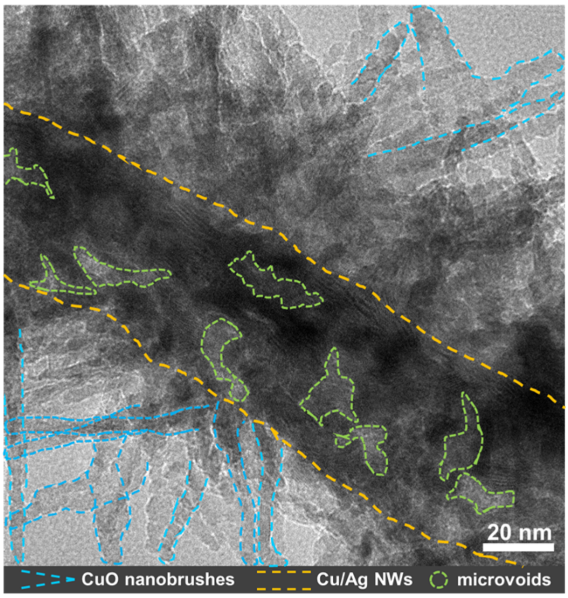

Figure S3. HRTEM images of Cu/Ag@CuO NWs-D. The bule, yellow, and green lines indicate the CuO brushes, Cu/Ag NWs, and microvoids in Cu/Ag@CuO NWs-D, respectively.

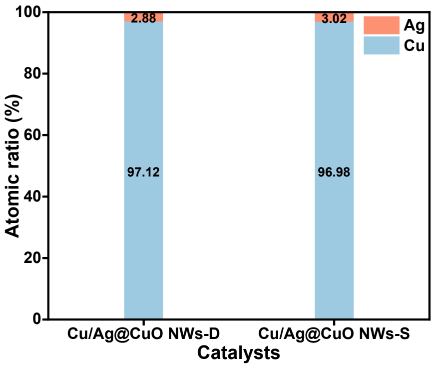

Figure S4. Atomic ratios between Cu and Ag of Cu/Ag@CuO NWs-D and Cu/Ag@CuO NWs-S from ICP analysis.

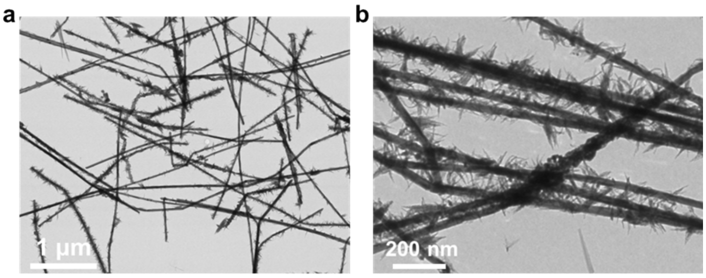

Figure S5. TEM images of Cu/Ag@CuO NWs-S with different magnifications.

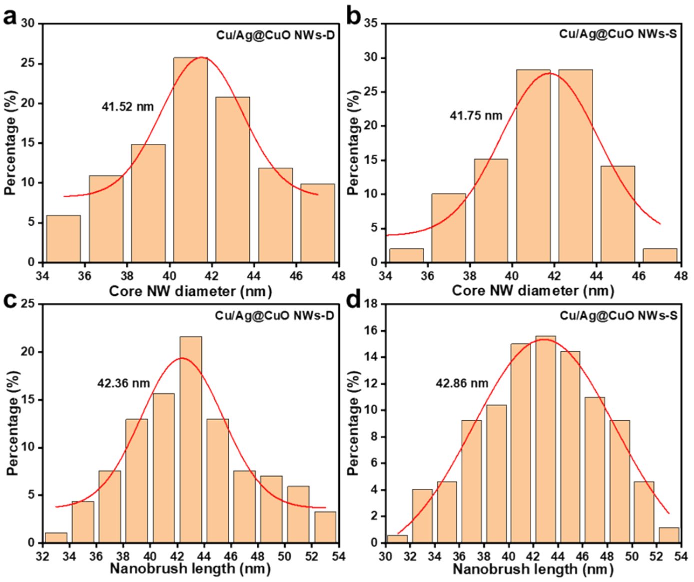

Figure S6. Histograms of the diameter of core NWs and length of outer nanobrushes for Cu/Ag@CuO NWs-D and Cu/Ag@CuO NWs-S. (a-b) Histograms of the diameter of core NWs. (c-d) Histograms of the length of outer nanobrushes.

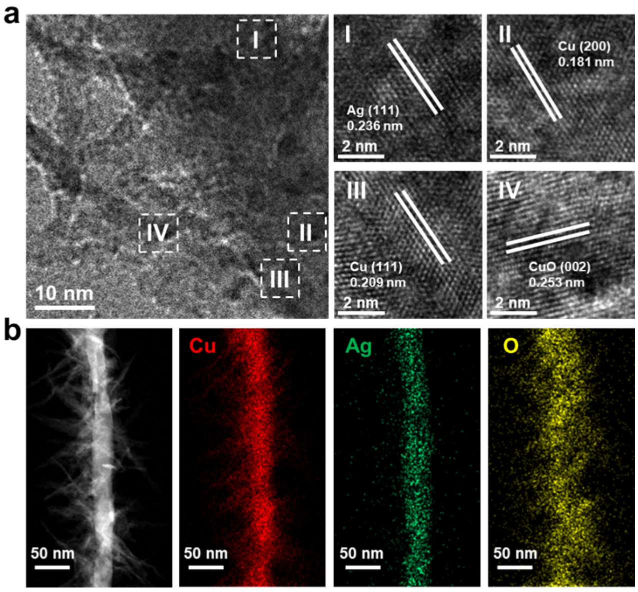

Figure S7. Morphological and structural characterizations of Cu/Ag@CuO NWs-S. (a) HRTEM images. (b) HADDF-STEM image and elemental mapping results.

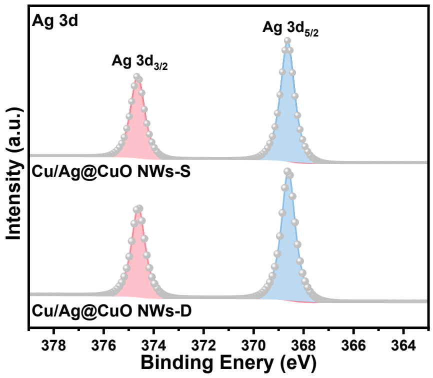

Figure S8. Ag 3d orbital spectra between Cu/Ag@CuO NWs-D and Cu/Ag@CuO NWs-S.

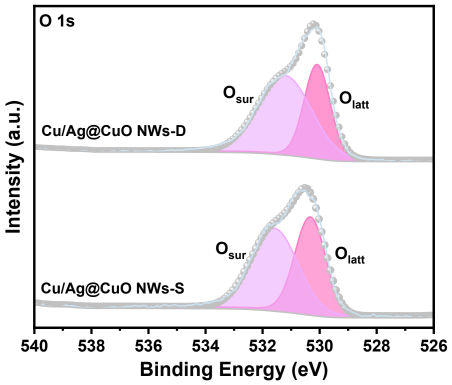

Figure S9. O 1s orbital spectra of Cu/Ag@CuO NWs-D and Cu/Ag@CuO NWs-S.

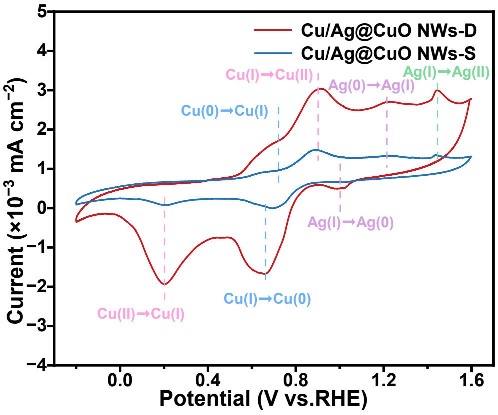

Figure S10. CV curves of Cu/Ag@CuO NWs-D and Cu/Ag@CuO NWs-S.

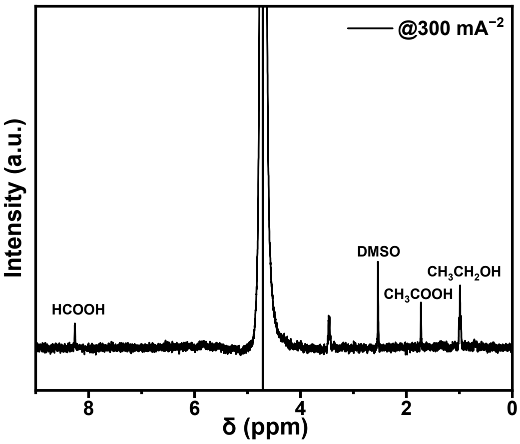

Figure S11. ^{1}H NMR spectra of the liquid products of Cu/Ag@CuO NWs-D catalysts at a current density of 300 mA cm^{-2}.

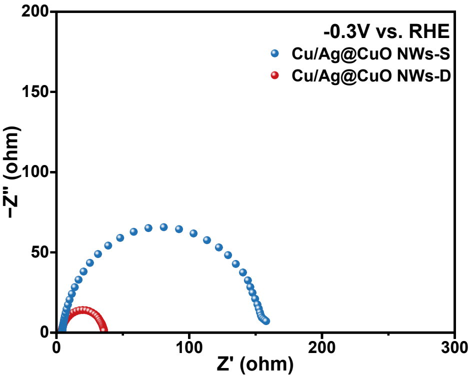

Figure S12. EIS spectra of Cu/Ag@CuO NWs-D and Cu/Ag@CuO NWs-S.

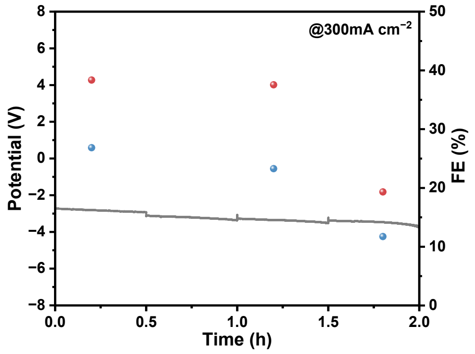

Figure S13. Durability of Cu/Ag@CuO NWs-S at 300 mA cm^{-2}.

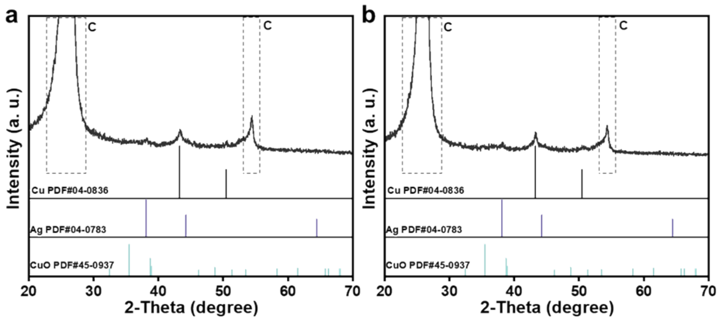

Figure S14. XRD patterns of Cu/Ag@CuO NWs-D. (a) Before CO_2RR tests. (b) After CO_2RR tests.

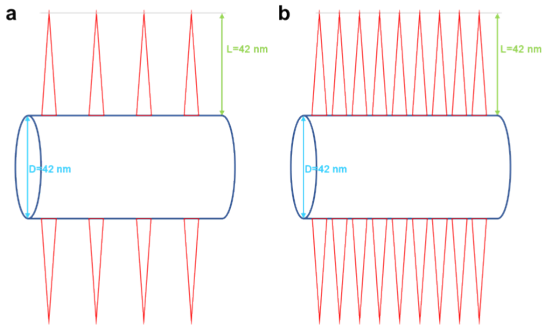

Figure S15. Geometric parameters of model construction. (a) Cu/Ag@CuO NWs-S. (b) Cu/Ag@CuO NWs-D.

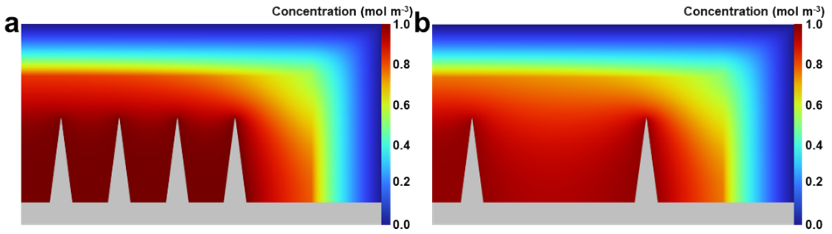

Figure S16. CO_2 concentration distributions in brushed NWs with different brush densities. (a) Densely brushed NW. (b). Sparsely brushed NW.

Table S1. Electrons transferred and standard reduction potentials for each product in CO_2RR.

Products	**Electrons transferred**	**Electrode reaction equations**	***E*⁰ (V *vs* RHE)**
CO	2	$CO_2 + 2H^+ + 2e^- \rightarrow CO + H_2O$	–0.1
CH_4	8	$CO_2 + 8H^+ + 8e^- \rightarrow CH_4 + H_2O$	0.17
HCOOH	2	$CO_2 + 2H^+ + 2e^- \rightarrow HCOOH$	–0.12
CH_3OH	6	$CO_2 + 6H^+ + 6e^- \rightarrow CH_3OH + H_2O$	0.03
C_2H_4	12	$2CO_2 + 12H^+ + 12e^- \rightarrow C_2H_4 + 4H_2O$	0.08
C_2H_6	14	$2CO_2 + 14H^+ + 14e^- \rightarrow C_2H_6 + 4H_2O$	0.16
C_2H_5OH	12	$2CO_2 + 12H^+ + 12e^- \rightarrow C_2H_5OH + 3H_2O$	0.09

REFRENCES

1. Q. Fu, Y. Li, H. Li, L. Xu, Z. Wang and S. Yu, *Langmuir*, 2019, **35**, 4364-4369.
2. J. Huang, X. Qiu, Z. Zhao, H. Zhu, Y. Liu, W. Shi, P. Liao and X. Chen, *Angew. Chem., Int. Ed.*, 2022, **61**, e202210985.